



**HAL**  
open science

## Controlled natural selection of soil microbiome through plant-soil feedback confers resistance to a foliar pathogen

Tetiana Kalachova, Barbora Jindřichová, Lenka Burketová, Cécile Monard,  
Manuel Blouin, Samuel Jacquiod, Eric Ruelland, Ruben Puga-Freitas

### ► To cite this version:

Tetiana Kalachova, Barbora Jindřichová, Lenka Burketová, Cécile Monard, Manuel Blouin, et al..  
Controlled natural selection of soil microbiome through plant-soil feedback confers resistance to a  
foliar pathogen. *Plant and Soil*, 2023, 485, pp.181-195. 10.1007/s11104-022-05597-w . hal-03735534

**HAL Id: hal-03735534**

**<https://institut-agro-dijon.hal.science/hal-03735534>**

Submitted on 8 Nov 2022

**HAL** is a multi-disciplinary open access archive for the deposit and dissemination of scientific research documents, whether they are published or not. The documents may come from teaching and research institutions in France or abroad, or from public or private research centers.

L'archive ouverte pluridisciplinaire **HAL**, est destinée au dépôt et à la diffusion de documents scientifiques de niveau recherche, publiés ou non, émanant des établissements d'enseignement et de recherche français ou étrangers, des laboratoires publics ou privés.

# Plant and Soil

## Controlled natural selection of soil microbiome through plant-soil feedback confers resistance to a foliar pathogen

--Manuscript Draft--

<b>Manuscript Number:</b>	PLSO-D-22-00365
<b>Full Title:</b>	Controlled natural selection of soil microbiome through plant-soil feedback confers resistance to a foliar pathogen
<b>Article Type:</b>	Research Article
<b>Keywords:</b>	controlled natural selection; plant-microbiome interactions; plant immunity; <i>Pseudomonas syringae</i> DC3000; salicylic acid; soil suppressiveness
<b>Abstract:</b>	<p><b>Background and aims</b> The rhizosphere microbiome has been shown to contribute to nutrient acquisition, protection against biotic and abiotic stresses and, ultimately, changes in the development and physiology of plants. Here, using a controlled natural selection approach, we followed the microbial dynamics in the soil of <i>Arabidopsis thaliana</i> infected with the foliar pathogen <i>Pseudomonas syringae</i> DC3000 ( Pst ).</p> <p><b>Methods</b> Plants were iteratively cultivated on a pasteurized soil inoculated with the soil microbial community of the previous iteration isolated from the rhizosphere of plants infected with Pst (pst-line) or not (mock-line). Modification of soil microbial communities was assessed through an amplicon-based metagenomic analysis targeting bacterial and fungal diversity. Plant fitness and transcript abundance of stress hormone related genes were also analysed.</p> <p><b>Results</b> At the tenth and eleventh iterations, we observed a reduction in disease severity of 81% and 85% in pst-lines as compared to mock-lines. These changes were associated with (i) a diminution of transcript abundance of salicylic acid related genes whereas jasmonic acid, ethylene or abscisic acid related genes were not modified and (ii) a shift in soil bacterial, but not in fungal, composition.</p> <p><b>Conclusions</b> Our study suggests that these changes in soil bacterial composition are mediated by plant-soil feedback in response to Pst and resulted in an activation of SA-related immune response in the plant. This supports the concept of applying plant-soil feedbacks to enhance soil suppressiveness against foliar pathogens.</p>

[Click here to view linked References](#)

1 **Title:**

2 Controlled natural selection of soil microbiome through plant-soil feedback confers resistance to a foliar pathogen

3

4 **Authors:**

5 Tetiana KALACHOVA<sup>1</sup>, Barbora JINDŘICHOVÁ<sup>1</sup>, Lenka BURKETOVÁ<sup>1</sup>, Cécile MONARD<sup>2</sup>, Manuel  
6 BLOUIN<sup>3</sup>, Samuel JACQUIOD<sup>3</sup>, Eric RUELLAND<sup>4</sup>, Ruben PUGA-FREITAS<sup>5</sup>

7

8 **Affiliations:**

9 <sup>1</sup>Institute of Experimental Botany of the Czech Academy of Sciences, Rozvojová 263, 165 02, Prague 6, Czech  
10 Republic

11 <sup>2</sup>Univ Rennes, CNRS, ECOBIO (Ecosystèmes, biodiversité, évolution) - UMR 6553, F-35000 Rennes, France

12 <sup>3</sup>Agroecologie, AgroSup Dijon, INRAE, Université Bourgogne Franche-Comte, Dijon, France

13 <sup>4</sup>UMR 7025 CNRS, GEC Génie Enzymatique et Cellulaire, Alliance Sorbonne Universités, Université de  
14 Technologie de Compiègne, F-60203 Compiègne, France

15 <sup>5</sup>Univ Paris Est Creteil, SU, CNRS, INRAE, IRD, Institute of Ecology and Environmental Sciences, IEES-Paris,  
16 F-94010 Creteil, France

17

18 **Corresponding author:**

19 Ruben Puga-Freitas

20 Université Paris Est Créteil, UMR 7618 - iEES

21 61, avenue du Général De Gaulle

22 94010 Créteil cedex – France

23 [ruben.puga-freitas@u-pec.fr](mailto:ruben.puga-freitas@u-pec.fr)

24 Telephone: +33(0)1 45 17 14 67

25

26

27

28

29

30

31 **Abstract**

32 *Background and aims*

33 The rhizosphere microbiome has been shown to contribute to nutrient acquisition, protection against biotic and  
34 abiotic stresses and, ultimately, changes in the development and physiology of plants. Here, using a controlled  
35 natural selection approach, we followed the microbial dynamics in the soil of *Arabidopsis thaliana* infected with  
36 the foliar pathogen *Pseudomonas syringae* DC3000 (*Pst*).

37 *Methods*

38 Plants were iteratively cultivated on a pasteurized soil inoculated with the soil microbial community of the  
39 previous iteration isolated from the rhizosphere of plants infected with *Pst* (pst-line) or not (mock-line).  
40 Modification of soil microbial communities was assessed through an amplicon-based metagenomic analysis  
41 targeting bacterial and fungal diversity. Plant fitness and transcript abundance of stress hormone related genes  
42 were also analysed.

43 *Results*

44 At the tenth and eleventh iterations, we observed a reduction in disease severity of 81% and 85% in pst-lines as  
45 compared to mock-lines. These changes were associated with (i) a diminution of transcript abundance of salicylic  
46 acid related genes whereas jasmonic acid, ethylene or abscisic acid related genes were not modified and (ii) a shift  
47 in soil bacterial, but not in fungal, composition.

48 *Conclusions*

49 Our study suggests that these changes in soil bacterial composition are mediated by plant-soil feedback in response  
50 to *Pst* and resulted in an activation of SA-related immune response in the plant. This supports the concept of  
51 applying plant-soil feedbacks to enhance soil suppressiveness against foliar pathogens.

52

53 **Keywords:** controlled natural selection; plant-microbiome interactions; plant immunity; *Pseudomonas syringae*  
54 DC3000; salicylic acid; soil suppressiveness

55

56 **Introduction**

57 Plant growth and development is strongly influenced by its environment. Among biotic factors, plant pathogens  
58 constitute a major threat to agriculture and food security around the world. The outcome of plant-pathogen  
59 interaction is governed by complex mechanisms resulting from long-term evolutionary processes but also from  
60 short-term responses not directly related to plant defence mechanisms and relying on the interaction with other

61 organisms or changes in the environment (Mitter et al. 2013; Pieterse et al. 2016). Plants shapes their rhizosphere  
62 through exuded carbon and other metabolites (Bais et al. 2006; Doornbos et al. 2012). Upon pathogen attack,  
63 changes in root exudates composition, often termed as “cry for help”, help to recruit beneficial organisms such as  
64 plant growth promoting microbes (PGPM) enabling the assemblage of a protective rhizosphere microbiome (Rolfe  
65 et al. 2019) which can, in return, influence plant resistance to pathogen infection. Several studies already showed  
66 that recruitment of soil microorganisms can lead to soil suppressiveness; *i.e.* to a low level of disease development  
67 even though a virulent pathogen and susceptible host are present (Weller et al. 2002). Soil suppressiveness has  
68 been demonstrated for many soilborne disease like take-all of wheat, *Fusarium* wilts, potato scab or apple replant  
69 disease. Soil suppressiveness, relies on the selection of beneficial organisms by the plants after repeated ulterior  
70 infections with the pathogen (Weller et al. 2002; Berendsen et al. 2012). However, the concept of soil  
71 suppressiveness is not restricted to soilborne pathogen and can be applied to other diseases even those caused by  
72 aboveground pathogens or pests (Pineda et al. 2017, 2020).

73

74 For soilborne pathogens, the soil microbial community might influence disease severity through direct impact on  
75 pathogenic microorganisms (*i.e.* through competition or production of antimicrobial compounds) thus influencing  
76 the disease incidence and severity (Berendsen et al. 2012). On the contrary, the impact of soil microbial  
77 community on aboveground disease severity is mediated by systemic changes in plant development and defence  
78 responses, such as systemic acquired resistance (SAR) and induced systemic resistance (ISR). In general, SAR is  
79 induced during a compatible host-pathogen interaction whereas ISR is elicited by PGPM. SAR and ISR acts  
80 antagonistically and relies on the activation of complex salicylic acid (SA) and jasmonic acid-ethylene (JA-ET)  
81 signalling pathways respectively, leading to localized and systemic defences (Pieterse et al. 2009). Activation of  
82 SAR or priming of ISR confers to the plant a broad-spectrum tolerance or resistance to ongoing and subsequent  
83 infections by pathogens and pests.

84

85 Thus, the soil microbiome has emerged as a key component of plant immunity, which has led to plant immunity  
86 no longer being seen as an innate genetic feature (Pieterse et al. 2016; Pineda et al. 2017). However, most of the  
87 studies about plant immunity to aboveground pathogens, conferred by beneficial microorganisms, focused on the  
88 impact of individual strains. Indeed, several soil microbial strains conferring a resistance in *Arabidopsis thaliana*  
89 to *Pseudomonas syringae* DC3000 (*Pst*) have already been identified (Mitter et al. 2013) and it was already shown  
90 that upon challenge by *Pst*, *A. thaliana* is able to recruit specific beneficial microbial strains to counteract

91 subsequent infections (Rudrappa et al. 2008; Yuan et al. 2018). Improvement of our knowledge, enhanced by the  
92 rapid development of inexpensive high-throughput DNA-sequencing, push towards integrating the role of soil  
93 microbiome in the understanding of plant immunity (Lemanceau et al. 2017).

94

95 In this work, through natural selection in a controlled environment (Conner 2003) we investigated the contribution  
96 of soil microbiome to *A.thaliana* adaptation to the foliar pathogen *Pst*. To do so, plants were divided in two lines,  
97 depending on whether they were (i) inoculated with *Pst* or (ii) a saline buffer. Then, a new batch of plants were  
98 iteratively cultivated on a pasteurized soil inoculated with the soil microbial community of the previous iteration  
99 (whether inoculated with *Pst* or not) during eleven iterations. This allowed us to mimic the dynamics of a soil  
100 microbial community exposed to successive monocultures infected or not with *Pst*. The inoculation of the foliar  
101 pathogen, in one line and not the other, aimed at testing if the pathogen can induce a modification of soil microbial  
102 community mediated by the plant. Modification of soil microbial communities by the plant in response to *Pst* was  
103 assessed through an amplicon-based metagenomic analysis targeting bacterial and fungal diversity. Plant fitness  
104 and transcript abundance of stress hormone related genes were also analysed to finely describe plant response to  
105 (i) *Pst* and (ii) changes in soil microbial composition.

106

## 107 **Materials and Methods**

### 108 *Experimental set-up*

109

110 *Arabidopsis thaliana* Col-0 seeds were surface-sterilized and stratified at 4°C for 2 days before sowing. Plants  
111 were cultivated in a growth chamber (Snijders, Netherlands) for 5 weeks at 22°C with daily cycles of 10 h light  
112 (100-130  $\mu\text{mol m}^{-2} \text{s}^{-1}$ ) and 14 h dark and 70% relative humidity. Initially (iteration 0), plants were cultivated in  
113 pots filled with a mixture of vermicompost, pasteurized natural sandy soil and pasteurized TS3 Aquasave substrate  
114 (pH=6.0, Recipe-No.: 316; Klasman-Deilmann, Lithuania) in 1:2:7 (v:v:v) ratio. Only vermicompost, originating  
115 from vegetable residues, was not pasteurized to provide a primary source of rich, diverse and abundant microbial  
116 community (Pathma and Sakthivel 2013). For the natural soil (cambisol with moor from CEREEP station, Saint-  
117 Pierre-Lès-Nemours, France), only the first 20 cm were sampled, excluding plant material before air-drying and  
118 sieving at 2 mm. Substrates were pasteurized for 72 h at 80 °C in a dry oven.

119

120 For the natural selection in a controlled environment experiment (Fig. 1), we established two “lines” (later denoted  
121 as pst-line and mock-line) of soil/plants microcosms (n=8), with one plant in each. After 4 weeks of growth, three  
122 leaves of each plant were inoculated with *Pst* or a saline buffer (10 mM MgCl<sub>2</sub>) for pst- and mock-line  
123 respectively. One week later, the disease severity on pst-lines was evaluated by quantification of *Pst* DC3000 in  
124 leaf tissues (as colony forming units, CFU). Since it was not technically possible to separate the soil from plant  
125 roots, the entire soil (including plants roots) from the different microcosm respective to their line, were retrieved  
126 and pooled. Pooling of the soil was done since it does not generates consistent inference bias (Allen et al. 2021)  
127 and eases preparation of new microcosms. After pooling, soil was mixed to be used as “inoculum” to inseminate  
128 the substrate for the next iteration. The cultivation substrate consisted of inoculum (pooled total soils from the  
129 previous iteration), pasteurized natural soil and pasteurized substrate TS3 in a ratio 1:2:7 (v:v:v). On these,  
130 *Arabidopsis* seeds were sown; this was performed for 11 iterations. Note that vermicompost, except for the first  
131 iteration, was not used for the rest of the controlled natural selection experiment as its physical and chemicals  
132 properties is difficult to standardize and characterize, which can lead to the introduction of non-controlled bias  
133 between two iterations. During iterations 1-6, plants were watered with demineralized water with no fertilizers;  
134 starting the 7th iteration plants were first watered with distilled water for 3 weeks and then with ¼ Steiner solution  
135 (Steiner 1961), due to the reinforcement of deficiency symptoms (symptoms that gradually got worse during the  
136 first generations). Substrate water content was kept at 60-80% of total water capacity (w:w). From the fourth to  
137 the last iteration, individual pictures of the plants were taken at 7 d.p.i. (days post inoculation with *Pst*). Total leaf  
138 area and rosette diameter was measured using ImageJ software (1.52v) and PHENOPSIS 3.0 ImageJ macro  
139 (Rymaszewski et al. 2018).

140

#### 141 *Inoculation with pathogens and evaluation of disease severity*

142

143 The inoculation with *Pseudomonas syringae* pv. *tomato* DC3000 (*Pst*) was performed according to literature  
144 (Katagiri et al. 2002) with the following modifications: bacteria were cultivated overnight on LB medium plates  
145 containing 50 µg.µl<sup>-1</sup> rifampicin. Bacteria were washed out from the plate and resuspended in 10 mM MgCl<sub>2</sub> up  
146 to OD<sub>600</sub>=0.0005. Four-week-old plants were syringe-infiltrated with the suspension: three leaves at the similar  
147 developmental stage (middle age leaves: 8th-9th-10th leaves) were infiltrated according to (Berens et al. 2019).  
148 At 7 d.p.i., three discs (6 mm in diameter) were sampled on three leaves from each plant and pooled for evaluation  
149 of disease severity. The discs were homogenized in 10 mM MgCl<sub>2</sub>, in a 2mL Eppendorf tube, with 1 g of 1.3 mm

150 silica beads using a FastPrep-24 instrument (MP Biomedicals, USA). The resulting homogenate was subjected to  
151 serial 10x dilutions and pipetted onto LB plates. Colonies were counted after 1–2 days of incubation at 28 °C.

152

### 153 *Plant gene expression*

154 Gene expression was monitored in plants of iterations 10 and 11, for both lines, 7 days post inoculation. Expression  
155 of defence-related genes was performed as in (Leontovyčová et al. 2019). Briefly, leaf discs (approximately 100  
156 µg fresh weight) were immediately frozen in liquid nitrogen. The tissue was homogenized similarly as for CFU  
157 quantification. Total RNA was isolated using Spectrum Plant Total RNA kit (Sigma-Aldrich, USA) and treated  
158 with a DNase DNA-free kit (Ambion, USA). Subsequently, 1 µg of RNA was converted into cDNA with M-MLV  
159 RNase H<sup>-</sup> Point Mutant reverse transcriptase (Promega Corp., USA) and an anchored oligo dT21 primer  
160 (Metabion, Germany). An equivalent of 6.25 ng of RNA was loaded into a 10-µl reaction with a SYBR Green  
161 qPCR Kit (ThermoFisher, USA). Gene expression was quantified by qPCR using a LightCycler 480 SYBR Green  
162 I Master kit and LightCycler 480 (Roche, Switzerland). The PCR conditions were 95 °C for 10 min followed by  
163 45 cycles of 95 °C for 10 s, 55 °C for 20 s, and 72 °C for 20 s. Melting curve analysis was then conducted. Relative  
164 gene expression was evaluated using  $\Delta\Delta C_t$ , where the genes of interest were normalized to the housekeeping gene  
165 *AtTIP41* and relative to the mock-line. Gene of interest are associated with stress-hormone signalling pathways:  
166 *PR1*, *PR2*, *PR5* and *ICS1* for SA-signalling pathway (Qi et al. 2018) ; *PDF1.2*, *AOS*, *LOX2* for JA pathway (Leon-  
167 Reyes et al. 2010); *ACS2*, *ERF1* for ethylene pathway (Wang et al. 2002); *ABII* and *LEA4-1* for ABA pathway  
168 (Dalal et al. 2009; Cao et al. 2017). A list of the primers is available in Supplementary Table S1.

169

### 170 *Soil DNA extraction and sequencing*

171 DNA was extracted from 500 mg of -20°C frozen soils following the (Griffiths et al. 2000) protocol with some  
172 modifications according to (Nicolaisen et al. 2008) and (Monard et al. 2013). Lysing Matrix E tubes (MP  
173 Biomedicals, California, USA) were used for the cell lysis and agitated at 30 m.s<sup>-1</sup> for 3 min in a bead beater.  
174 Glycogen (0.1 mg) was added to precipitate nucleic acids for 2 h at 4 °C that were subsequently pelleted by  
175 centrifugation at 18 000 g for 30 min at 4 °C. Nucleic acids were resuspended in 50 µl of DNase–RNase-free  
176 water.

177

178 Bacteria and fungi libraries were constructed according to the Illumina protocol "16S metagenomic sequencing  
179 library preparation" using a two steps polymerase chain reaction (PCR) approach. The following primer sets were



180 used for bacteria and fungi: 341F (5'-CCTACGGGNGGCWGCAG-3') and 785R (5'-  
181 GACTACHVGGGTATCTAATCC-3') (Klindworth et al. 2013), ITS1f (5'-CTTGGTCATTTAGAGGAAGTAA-  
182 3') (Gardes and Bruns 1993) and ITS2 (5'-GCTGCGTTCTTCATCGATGC-3') (White et al. 1990), respectively.  
183 Each primer set contains a supplementary sequence, the overhang adapter: forward overhang (5'-  
184 TCGTCGGCAGCGTCAGATGTGTATAAGAGACAG-3') and reverse overhang (5'-  
185 GTCTCGTGGGCTCGGAGATGTGTATAAGAGACAG-3'). PCRs were conducted in 25 µl containing each  
186 bacterial or fungal primer (0.2µM), 12.5µl 2X TransTaq® Hifi PCR SuperMix II (TransGen Biotech, Beijing,  
187 China), 2 µl of tenfold diluted DNA and ultrapure water to reach the final volume. The amplification conditions  
188 were as followed: for bacteria, 3 min at 95°C, 25 cycles of 30 s at 95°C, 30 s at 55°C and 30 s at 72°C and a final  
189 5 min extension step at 72°C; for fungi, 4 min at 95°C, followed by 30 cycles of 30 s at 95°C, 30 s at 56°C and  
190 30 s at 72°C and a final 10 min extension step at 72°C. Two independent PCR replicates were performed for each  
191 sample, the PCR products were pooled and purified using the Agencourt® AMPure® XP beads system. The  
192 second PCR reaction attached specific indexes (i5, i7) to identify each sample and the Illumina sequencing  
193 adapters (P5, P7) using the Nextera XT index kit, 1X KAPA2G Robust mastermix (Kapa Biosystems,  
194 Wilmington, Massachusetts, USA) and the SmartChip technology (Wafergen, Fremont, USA). The amplification  
195 conditions consisted in 3 min at 95°C, followed by 8 cycles of 30 s at 95°C, 30 s at 55°C and 30 s at 72°C, and a  
196 final 5 min extension step at 72°C. After the polymerase chain reactions, pooled amplicons were collected from  
197 the chip(s) via centrifugation using single-use components supplied in the SmartChip TE Collection Kit and were  
198 purified with the Agencourt® AMPure® XP beads system.

199 The amplified products of bacteria and fungi were quantified by qPCR (light cycler 480, Roche, Meylan, France)  
200 with, per well, 2.67 µl of PCR product, 4 µl of premix containing 2X of KAPA SYBR FAST qPCR Master Mix  
201 (KAPA library quantification kit for illumina, Kapa Biosystems, Wilmington, USA) and the Illumina primers P5  
202 (5'-AATGATACGGCGACCACCGA-3') and P7 (5'-CAAGCAGAAGACGGCATAACGA-3'). The qPCR  
203 program consisted in 3 min at 95°C, followed by 45 cycles of 30 s at 95°C, 45 s at 60°C, 20 s at 72°C and a final  
204 melting curve step of 0.05 s at 95°C, 1 min at 65°C and an increase of 0.06°C/s from 65°C to 97°C. Then, the  
205 amplified products were combined in a unique pool in equimolar ratio and sequenced using 2x250 bp paired-end  
206 Illumina MiSeq with 15% PhiX at the 'Human and Environmental Genomic' platform (Rennes, France).

207

208 *Amplicon-based metagenomic analysis*

209 The sequence reads obtained after sequencing were analysed using Find Rapidly OTUs with Galaxy Solution  
210 (FROGS) pipeline at the Genotoul platform following the standard operation procedure. Unless specified  
211 otherwise, data were processed using default parameters. Briefly, reads were pre-processed to filter out sequences  
212 without primers, that are too small or of poor quality (ambiguous bases) and to trim the primers. Sequences were  
213 clustered using the Swarm algorithm (Mahé et al. 2014). Chimera sequences were detected and then removed.  
214 Clustered OTU were filtered to remove OTU that are present in at least two samples and containing at least  
215 0.00005% of all sequences. Taxonomy was assigned to OTU using SILVA (release 132) and UNITE (release 7.1)  
216 as reference database for 341F/785R and ITS1F/ITS2 reads respectively.

217

### 218 *Statistical and microbial community analyses*

219 All statistical analyses were performed using the R software (R Core Team 2020). Bacterial and fungal  
220 communities diversity analyses were performed with the R packages Phyloseq (McMurdie and Holmes 2013).  
221 Data were rarefied to 9220 and 14753 sequences/samples for bacteria (341F/785R) and fungi (ITS1F/ITS2) reads,  
222 respectively. Correspondence analysis was performed with the *ade4* package (Thioulouse et al. 2018). To identify  
223 the OTUs the most associated with pst- and mock- lines, the 200 OTUs with the highest absolute contribution to  
224 the first axis were isolated. A specific subset of OTUs associated to the pst-line and the mock-line was obtained  
225 by filtering on the data of the eleventh iteration. For the pst-line, only the OTUs detected in all three replicates of  
226 the pst-line and not detected in at least one replicate of the mock-line were kept. For the mock-line, only the OTUs  
227 detected in all three replicates of the mock-line and not detected in at least one replicate of the pst-line were kept.  
228 This provided a specific set of 78 and 34 OTUs for pst- and mock-line respectively.

229

## 230 **Results**

### 231 *Plant resistance to Pst but not growth increased between pst- and mock-line*

232 To determine the influence of the iterative inoculation of plants with a leaf pathogen on the associated rhizosphere  
233 microbial communities, we performed a natural selection in a controlled environment experiment (Fig. 1). One  
234 week after infiltration with *Pst*, inoculated leaves showed strong symptoms of infection (necrotic lesions  
235 surrounded by diffuse chlorosis) (Fig. 2a). On the contrary, for plants infiltrated with saline buffer, no leaf damage  
236 nor necrosis was observed (Fig. 2a). Plant growth (Fig. 2b), monitored through the projected leaf area (PLA)  
237 showed a progressive decrease starting from the fourth iteration up to the eighth. At the ninth iteration, PLA  
238 increased to values close to that of the fourth iteration and remained steady, up to the last iteration. For the fourth

239 and seventh iteration, we observed a significant difference in PLA between the plants of the pst- and the mock-  
240 line (p-value < 0.05, Wilcoxon test). No significant differences (p-value > 0.05, Wilcoxon test) were observed for  
241 the other iterations. At the tenth and eleventh iterations, PLA of plants in the mock-line, inoculated with *Pst* did  
242 not differ from plants in the pst-line (Fig. 1b). For both 10th and 11th iterations in which additional plant of the  
243 mock line were used to compare plant susceptibility to the pathogen in both pst- and mock-lines, the number of  
244 bacteria was significantly lower (p-value < 0.05, Wilcoxon test) in plants from the pst-line versus those of the  
245 mock-line: -81% (Fig. 2c) and -85% (Supplementary Fig. S1) for iteration 10 and 11, respectively.

246

#### 247 *Gene expression*

248 Among all tested genes, we detected a significant (p-value < 0.05, Wilcoxon test) differences between lines only  
249 in expression of genes associated with the SA-pathway (*PR1*, *PR2* and *PR5*) and SA biosynthesis gene *ICS1* (Fig.  
250 3 for i10 and Supplementary Fig. S2 for i11). The SA-related response was stronger in the mock line than in the  
251 pst-line in two subsequent iterations. For the other genes, no significant differences (p-value > 0.05, Wilcoxon  
252 test) in transcripts levels was detected between mock- and pst-lines (Fig. 3 for i10 and Supplementary Fig. S2 for  
253 i11).

254

#### 255 *Rhizosphere microbiome community dynamics*

256 Soil bacterial and fungal diversity, assessed through the phylogenetic analysis of 16S rRNA and ITS gene  
257 amplicons, was strongly impacted at first by the experimental setup (Supplementary Fig. S3). For bacterial  
258 diversity, species richness almost doubled the first iteration, going from 365 to 645 and 698 for mock and pst-line  
259 respectively. Species richness then stabilized around 840 for the following iterations (three times more as  
260 compared to initial soil). A similar pattern was observed for fungal diversity, with an increased species richness  
261 from 28 to 110 for both mock and pst-line in the first iteration. Species richness strongly varied the next iterations,  
262 before decreasing from the sixth iteration. For the last three iterations, species richness was around 40 (1.5 times  
263 more as compared to initial soil). For bacterial communities, Shannon H-index, followed a similar pattern than  
264 species richness with an initial increase from 5 to 5.6 and remained stable for the following iterations. For fungal  
265 communities, Shannon H-index remained stable the first four iterations (around 2.4) before decreasing and  
266 reaching 1.3 the last iterations.

267

268 When comparing bacterial (Fig. 4a) and fungal (Fig. 4b) communities between two successive iterations within  
269 the same line (*i.e.* legacy effect), we observe that for both soil lines, shift in beta-diversity was the highest between  
270 the initial soil and the first iteration (i0-i1), with values around 0.63 and 0.72 for bacterial and fungal communities  
271 respectively. Between successive iteration beta-diversity then decreased in both lines through the experiment and  
272 remained low from the sixth to the last iteration for both lines (mock and pst) and bacterial and fungal  
273 communities. When compared, the dissimilarity in bacterial composition between the mock and pst-line for the  
274 same iteration (*i.e.* inter treatment dissimilarity), increased between the first and fourth iteration and then remained  
275 stable at high values till the end of the iteration process (Fig. 4c). Dissimilarity between bacterial communities of  
276 the same line (*i.e.* intra treatment dissimilarity) also increased during the first three iterations and then decreased  
277 and remained low for both mock- and pst-line (Fig. 4c). From the third and up to the last iteration, inter-treatment  
278 (mock *vs.* pst) dissimilarity was higher than the intra-treatment (mock or pst) dissimilarity. For fungal  
279 communities (Fig. 4d), an increase in both intra and inter-treatment dissimilarity was also observed in the first  
280 iterations. Intra and inter dissimilarity then decreased from i3 up to i11, with only a brief increase at i10 for the  
281 pst-line community (thus increasing the inter-treatment dissimilarity). As fungal communities did not appear to  
282 be impacted by *Pst*, we only consider bacterial communities in further analyses.

283

#### 284 *Bacterial sub-community differences between pst- and mock- lines*

285

286 Correspondence analysis (CA, Fig. 5a) confirmed the strong influence of the experimental setup during the first  
287 iterations, as already shown by between successive iteration beta-diversity (Fig. 4a). In the CA map, samples are  
288 distributed according to their iterations, with samples from initial soil (i0) and first iteration (i1) contributing the  
289 most to both the first and second axis. Besides, the bacterial communities of i0 and i1 samples show a great  
290 divergence with those of following iterations (i2 to i11). The last iterations (i5 to i11) are joined on the CA map  
291 and contribute poorly to the first and second axis, showing a relative stabilization of microbial community  
292 structure (Fig. 4a and 4c). To have a better view of what happens for the last iterations, CA was performed using  
293 only the samples corresponding to the last four iterations (i8 to i11) (Fig. 5b). It shows a strong impact of the *Pst*  
294 inoculation on microbiome composition as samples are distributed along the first axis according to the line (pst or  
295 mock), with samples of the mock-line being mainly on the left and pst-line on the right. Interestingly, the second  
296 axis separates the samples according to their iterations, with samples of pst-line and mock-line for a given iteration  
297 nearly mirroring according to the second axis.

298

299 Following CA, we selected the OTUs that contribute the most, positively, or negatively, to the first axis. We  
300 identified (Fig. 6a) a specific set of 78 OTUs whose abundance increased through the iterative process in the pst-  
301 line but not in the mock line. These OTUs which represented less than 1 % of the relative abundance during the  
302 first two iterations represented up to 11% in the last iteration. These OTUs were mostly related to the phyla  
303 Proteobacteria (4 %), Planctomycetes (3 %) and Bacteroides (1.8 %) (Fig. 6a) with families such as  
304 *Tepidisphaeraceae*, *Xanthobacteraceae* and *Caedibacteraceae* being the most abundant in pst-line but not in  
305 mock-line (Supplementary Table S2 and S3). In the mock-line, the abundance of these OTUs did not change and  
306 has remained broadly close to 1% during the whole experiment. In soils of the mock-line, we also identified a  
307 specific set of 34 OTUs (Fig. 6b) which abundance increased during the iterative process. These OTUs represented  
308 less than 2% of the relative abundance during the first two iterations and up to 4.4 % in the last iteration. These  
309 OTUs are mostly related to the phyla Proteobacteria (2.1 %) and Bacteroides (1.1 %). A decrease in the abundance  
310 of these OTUs was observed in soils iteratively exposed to *Pst*. They represented up to 2.5 % of the total abundance  
311 in the first iterations and dropped close to 0.5% in the last iterations.

312

### 313 **Discussion**

#### 314 *Susceptibility to Pst decreased in the line iteratively exposed to Pst*

315 Iterative exposure of soil to plants inoculated with *Pst* did not significantly impact plant growth and development  
316 as there were no differences between the mock- and pst-lines during the iterative process (Fig. 2b). However, from  
317 the 4th to the 8th iteration, plant growth decreased. This might be due to an uncontrolled environmental factor.  
318 This phenomenon might have been accentuated by the small pot size, chosen to maximize the volume occupied  
319 by the roots to increase the rhizosphere (and so the interactions with soil microorganisms). Fertilization of the  
320 plants with a Steiner solution, started at the seventh iteration, might have allowed them to overcome this effect in  
321 the last iterations (i9 to i11). Although no significant differences were observed between mock- and pst-lines  
322 regarding plant growth (except for iteration 4 and 7), plant susceptibility to *Pst* was strongly modulated. Plants  
323 grown on soils of iteration 10, *i.e.* soil microbiome that has been ten times consecutively exposed to plants exposed  
324 to *Pst*, appeared far less susceptible to the disease. This was shown by a decrease of 81 and 85 % in *Pst* density  
325 in pst-line as compared with mock-line, at iterations 10 and 11 respectively. Interestingly, the increased resistance  
326 in pst-line observed at the tenth and eleventh iterations was coupled with the lower transcription of *PR1*. *PR1* is  
327 the canonical SA-responsive gene, used as an indicator of the triggering of SA signalling (Janda and Ruelland

328 2015). During *Pst* infection, SA signalling (i.e. *PR1* expression) turns on rapidly (16-24 hpi) peaking around 48  
329 hpi and gradually decreasing afterwards (De Vos et al. 2005; Yang et al. 2015). The increased resistance at 7 dpi  
330 in pst-line, correlated with lower SA signalling at this very moment, might indicate that defence mechanisms were  
331 activated in pst-line allowing the plant to overcome the infection faster. This activation could be linked to the  
332 presence of PGPM or molecules inducing SA related defence mechanisms (Pieterse et al. 2009). For example, *Pst*  
333 infection resistance in *A. thaliana* plants induced by the PGPM *Bacillus cereus* AR156 and *Burkholderia*  
334 *phytofirmans* PsJN (Bp) is associated to higher levels of transcripts of SA related genes in the first stage of the  
335 infection but lower in the late stage of the infection as compared to non-elicited plants (Niu et al. 2011; Su et al.  
336 2017). On conditioned soils (i.e. by growing in the same soil, multiple generations of *A. thaliana* inoculated  
337 aboveground with *Pst*), a similar decrease of endogenous SA level was observed (Yuan et al. 2018). Conversely,  
338 we did not detect any significant differences in transcript abundance of JA-responsive (*PFDI.2*) or biosynthetic  
339 genes (*AOS*, *LOX2*), ET- (*ACS2*, *ERF1*) or ABA-associated (*ABI1*, *LEA4-1*) genes between pst- and mock-lines,  
340 consistently with the antagonistic role of those hormones (Robert-Seilaniantz et al. 2011). Even if we did not see  
341 any significant differences for other hormones than SA, involvement of other hormones like JA or ET cannot be  
342 totally excluded. There is more and more evidence of a strong interplay of plant hormones, even between  
343 antagonistic ones, to finely tune plant response to pathogens, with often a time-lagged regulation of hormones  
344 levels (Liu et al. 2016; Klessig et al. 2018). This interplay between plant hormones plays an important role in  
345 plant-microbiome interactions as several soil organisms can interact with plant hormone signalling, modulating  
346 *in fine* hormone levels and thus plant response to pathogens (Hase et al. 2003; Dodd et al. 2010; Puga-Freitas and  
347 Blouin 2015; Trivedi et al. 2021).

348

#### 349 *Natural selection by the Pst-infected plants of a soil microbiome alleviating Pst associated symptoms*

350 Since new seeds were sown at the beginning of each iteration, and a fresh *Pst* inoculum was used for each  
351 infection, the effects observed on plant susceptibility could not be attributed to plant adaptation to the pathogen  
352 neither to the pathogen adaptation, as already observed in other studies (Luna et al. 2012; Meaden and Koskella  
353 2017). Modulation of plant susceptibility to *Pst* on the final iterations (i10 and i11) can therefore only be due to  
354 changes in soil biological, physical or chemical properties as a small proportion of soil was transferred between  
355 iterations (10 % of final volume). However, changes in soil physical and chemical properties were limited as soil  
356 was destructured by breaking aggregates between two successive iterations and plants were fertilized using a  
357 nutritive solution after the seventh iteration. Soil biological properties, especially bacterial dynamics, thus

358 appeared as a key element in the alleviation of *Pst* susceptibility in our experiment. Bacterial and fungal  
359 communities tended to stabilize along the iterative process (Fig. 4a) as the legacy effect increases (*i.e.* for a same  
360 line, divergence between two successive iterations tended to decrease). Aboveground inoculation with *Pst*  
361 impacted bacterial communities (Fig. 4c) but not fungal communities (Fig. 4d). Enrichment of rhizospheric  
362 microorganisms following infections has been extensively reported in suppressive soils (Raaijmakers and Mazzola  
363 2016; Cordovez et al. 2019). On these soils, suppression of a specific subset of disease caused by soilborne  
364 phytopathogenic fungi, oomycetes, bacteria or nematodes is generally observed. It has been strongly suggested  
365 that this protection is mediated by changes in the soil microbiome composition (Sanguin et al. 2009; Mendes et  
366 al. 2011; Raaijmakers and Mazzola 2016). In our study, the iterative cultivation of plants on a pasteurized soil  
367 inoculated with the soil microbial community of the previous iteration (whether inoculated with *Pst* or not) acted  
368 as a driving force to shape soil microbiome composition. This resulted in the selection by the plant, likely through  
369 its root exudates (Bais et al. 2006; Rudrappa et al. 2008; Yuan et al. 2018), of bacterial families such as  
370 *Burkholderiaceae*, *Caulobacteraceae*, *Sphingobacteriaceae* and *Sphingomonadaceae* (Supplementary Table S2),  
371 that helped the plants to overcome the infection as already shown in other pathosystems (Chapelle et al. 2016).  
372 After ten iterations, this microbial community is stable and can be therefore transferred to a new soil. For soilborne  
373 pathogens, it have been demonstrated that specific suppressiveness of soils can be transferred to conducive ones  
374 by mixing small amounts (1 to 10 % w/w) of the suppressive soil into the conducive soil (Mendes et al. 2011;  
375 Raaijmakers and Mazzola 2016). A similar mixing ratio seems to be also valid for diseases aboveground pathogens  
376 as shown in our study comforting that the concept of soil suppressiveness can be extended to aboveground  
377 pathogen or pests. However, the soil community trait selected by the plants differs according to the type of  
378 pathogen (soilborne or foliar). For soilborne pathogens, modifications induced by soil microbiome likely lead to  
379 changes in physicochemical soil properties and activation of specific antagonistic traits that restrict pathogen  
380 infection such as production of antimicrobial compounds or siderophores (Raaijmakers et al. 2009; Schlatter et al.  
381 2017). For foliar pathogens, as in our study, such direct impact of soil microbiome on the pathogen seems unlikely.  
382 Here, the mechanisms involved is therefore systemic and indirect, and relies extensively in the modulation by soil  
383 microbiome of the plant immunity related to SA homeostasis as demonstrated in the current and previous studies  
384 (Yuan et al. 2018).

385

386 To conclude, active shaping of soil microbiome by plant-soil feedbacks during pathogen infection allows to recruit  
387 a stable microbiome leading to a reduction in the susceptibility to the disease. This indirect mechanism could rely

388 upon a systemic response induced by soil organisms and is mediated in the plant through SA signalling. The use  
389 of similar controlled natural selection approaches could lead to the development of new agricultural strategies as  
390 the complex microbiomes obtained can be introduced to other soils via soil transplantation. Such approach needs  
391 to be associated to breeding strategies that optimize interactions with beneficial microbes, as plant interaction with  
392 soil organisms is a major driver of terrestrial ecosystems functioning.

393

#### 394 **Acknowledgements**

395 We thank Sophie Michon-Coudouel and Romain Causse-Védrine from the EcogenO Platform (OSUR, France)  
396 for the preparation of the sequencing libraries and the sequencing. We are also grateful to the genotoul  
397 bioinformatics platform Toulouse Occitanie (Bioinfo Genotoul,  
398 <https://doi.org/10.15454/1.5572369328961167E12>) for providing computing resources and to Dr. Aleš Hanč from  
399 the Czech University of Life Sciences (Prague), for providing the vermicompost.

400

#### **References**

Allen WJ, Sapsford SJ, Dickie IA (2021) Soil sample pooling generates no consistent inference bias: a meta-analysis of 71 plant–soil feedback experiments. *New Phytologist* 231:1308–1315.

<https://doi.org/10.1111/nph.17455>

Bais HP, Weir TL, Perry LG, et al (2006) The role of root exudates in rhizosphere interactions with plants and other organisms. *Annual review of plant biology* 57:233–66.

<https://doi.org/10.1146/annurev.arplant.57.032905.105159>

Berendsen RL, Pieterse CMJ, Bakker PAHM (2012) The rhizosphere microbiome and plant health. *Trends in Plant Science* 17:478–486. <https://doi.org/10.1016/j.tplants.2012.04.001>

Berens ML, Wolinska KW, Spaepen S, et al (2019) Balancing trade-offs between biotic and abiotic stress responses through leaf age-dependent variation in stress hormone cross-talk. *Proceedings of the National Academy of Sciences of the United States of America* 116:2364–2373.

<https://doi.org/10.1073/pnas.1817233116>

Cao M-J, Zhang Y-L, Liu X, et al (2017) Combining chemical and genetic approaches to increase drought resistance in plants. *Nature Communications* 8:1183. <https://doi.org/10.1038/s41467-017-01239-3>



- Chapelle E, Mendes R, Bakker PAHM, Raaijmakers JM (2016) Fungal invasion of the rhizosphere microbiome. *The ISME Journal* 10:265–268. <https://doi.org/10.1038/ismej.2015.82>
- Conner JK (2003) Artificial Selection: A Powerful Tool for Ecologists. *Ecology* 84:1650–1660
- Cordovez V, Dini-Andreote F, Carrión VJ, Raaijmakers JM (2019) Ecology and evolution of plant microbiomes. *Annual Review of Microbiology* 73:69–88. <https://doi.org/10.1146/annurev-micro-090817-062524>
- Dalal M, Tayal D, Chinnusamy V, Bansal KC (2009) Abiotic stress and ABA-inducible Group 4 LEA from *Brassica napus* plays a key role in salt and drought tolerance. *Journal of Biotechnology* 139:137–145. <https://doi.org/10.1016/j.jbiotec.2008.09.014>
- De Vos M, Van Oosten VR, Van Poecke RMP, et al (2005) Signal Signature and Transcriptome Changes of *Arabidopsis* During Pathogen and Insect Attack. *Molecular Plant-Microbe Interactions* 18:923–937. <https://doi.org/10.1094/MPMI-18-0923>
- Dodd ICC, Zinovkina NY, Safronova VII, Belimov AAA (2010) Rhizobacterial mediation of plant hormone status. *Annals of Applied Biology* 157:361–379. <https://doi.org/10.1111/j.1744-7348.2010.00439.x>
- Doornbos R, van Loon L, Bakker P (2012) Impact of root exudates and plant defense signaling on bacterial communities in the rhizosphere. A review. *Agronomy for Sustainable Development* 32:227–243. <https://doi.org/10.1007/s13593-011-0028-y>
- Gardes M, Bruns TD (1993) ITS primers with enhanced specificity for basidiomycetes - application to the identification of mycorrhizae and rusts. *Molecular Ecology* 2:113–118. <https://doi.org/10.1111/j.1365-294X.1993.tb00005.x>
- Griffiths RI, Whiteley AS, O'Donnell AG, Bailey MJ (2000) Rapid method for coextraction of DNA and RNA from natural environments for analysis of ribosomal DNA- and rRNA-based microbial community composition. *Applied and Environmental Microbiology* 66:5488–5491. <https://doi.org/10.1128/AEM.66.12.5488-5491.2000>
- Hase S, Van Pelt JA, Van Loon LC, Pieterse CMJ (2003) Colonization of *Arabidopsis* roots by *Pseudomonas fluorescens* primes the plant to produce higher levels of ethylene upon pathogen infection. *Physiological and Molecular Plant Pathology* 62:219–226. [https://doi.org/10.1016/S0885-5765\(03\)00059-6](https://doi.org/10.1016/S0885-5765(03)00059-6)
- Janda M, Ruelland E (2015) Magical mystery tour: Salicylic acid signalling. *Environmental and Experimental Botany* 114:117–128. <https://doi.org/10.1016/j.envexpbot.2014.07.003>

- Katagiri F, Thilmony R, He SY (2002) The Arabidopsis Thaliana-Pseudomonas Syringae Interaction. The Arabidopsis Book 1:e0039. <https://doi.org/10.1199/tab.0039>
- Klessig DF, Choi HW, Dempsey DA (2018) Systemic Acquired Resistance and Salicylic Acid: Past, Present, and Future. *Molecular Plant-Microbe Interactions* 31:871–888. <https://doi.org/10.1094/MPMI-03-18-0067-CR>
- Klindworth A, Pruesse E, Schweer T, et al (2013) Evaluation of general 16S ribosomal RNA gene PCR primers for classical and next-generation sequencing-based diversity studies. *Nucleic Acids Research* 41:1–11. <https://doi.org/10.1093/nar/gks808>
- Lemanceau P, Blouin M, Muller D, Moëgne-Loccoz Y (2017) Let the Core Microbiota Be Functional. *Trends in Plant Science* xx: <https://doi.org/10.1016/j.tplants.2017.04.008>
- Leon-Reyes A, Van der Does D, De Lange ES, et al (2010) Salicylate-mediated suppression of jasmonate-responsive gene expression in Arabidopsis is targeted downstream of the jasmonate biosynthesis pathway. *Planta* 232:1423–1432. <https://doi.org/10.1007/s00425-010-1265-z>
- Leontovyčová H, Kalachova T, Trdá L, et al (2019) Actin depolymerization is able to increase plant resistance against pathogens via activation of salicylic acid signalling pathway. *Scientific Reports* 9:1–10. <https://doi.org/10.1038/s41598-019-46465-5>
- Liu L, Sonbol F-M, Huot B, et al (2016) Salicylic acid receptors activate jasmonic acid signalling through a non-canonical pathway to promote effector-triggered immunity. *Nature Communications* 7:13099. <https://doi.org/10.1038/ncomms13099>
- Luna E, Bruce TJA, Roberts MR, et al (2012) Next-Generation Systemic Acquired Resistance. *Plant Physiology* 158:844–853. <https://doi.org/10.1104/pp.111.187468>
- Mahé F, Rognes T, Quince C, et al (2014) Swarm: Robust and fast clustering method for amplicon-based studies. *PeerJ* 2014:1–13. <https://doi.org/10.7717/peerj.593>
- McMurdie PJ, Holmes S (2013) Phyloseq: An R Package for Reproducible Interactive Analysis and Graphics of Microbiome Census Data. *PLoS ONE* 8:. <https://doi.org/10.1371/journal.pone.0061217>
- Meaden S, Koskella B (2017) Adaptation of the pathogen, *Pseudomonas syringae*, during experimental evolution on a native vs. alternative host plant. *Molecular Ecology* 26:1790–1801. <https://doi.org/10.1111/mec.14060>
- Mendes R, Kruijt M, de Bruijn I, et al (2011) Deciphering the rhizosphere microbiome for disease-suppressive bacteria. *Science (New York, NY)* 332:1097–100. <https://doi.org/10.1126/science.1203980>

- Mitter B, Brader G, Afzal M, et al (2013) Advances in Elucidating Beneficial Interactions Between Plants, Soil, and Bacteria. In: Sparks DLBT-A in A (ed). Academic Press, pp 381–445
- Monard C, Gantner S, Stenlid J (2013) Utilizing ITS1 and ITS2 to study environmental fungal diversity using pyrosequencing. *FEMS Microbiology Ecology* 84:165–175. <https://doi.org/10.1111/1574-6941.12046>
- Nicolaisen MH, Bælum J, Jacobsen CS, Sørensen J (2008) Transcription dynamics of the functional *tfdA* gene during MCPA herbicide degradation by *Cupriavidus necator* AEO106 (pRO101) in agricultural soil. *Environmental Microbiology* 10:571–579. <https://doi.org/10.1111/j.1462-2920.2007.01476.x>
- Niu D-D, Liu H-X, Jiang C-H, et al (2011) The Plant Growth-Promoting Rhizobacterium *Bacillus cereus* AR156 Induces Systemic Resistance in *Arabidopsis thaliana* by Simultaneously Activating Salicylate- and Jasmonate/Ethylene-Dependent Signaling Pathways. *Molecular Plant-Microbe Interactions* 24:533–542. <https://doi.org/10.1094/MPMI-09-10-0213>
- Pathma J, Sakthivel N (2013) Molecular and functional characterization of bacteria isolated from straw and goat manure based vermicompost. *Applied Soil Ecology* 70:33–47. <https://doi.org/10.1016/j.apsoil.2013.03.011>
- Pieterse CMJ, de Jonge R, Berendsen RL (2016) The Soil-Borne Supremacy. *Trends in Plant Science* 21:171–173. <https://doi.org/10.1016/j.tplants.2016.01.018>
- Pieterse CMJ, Leon-Reyes A, Van der Ent S, Van Wees SCM (2009) Networking by small-molecule hormones in plant immunity. *Nature Chemical Biology* 5:308–316. <https://doi.org/10.1038/nchembio.164>
- Pineda A, Kaplan I, Bezemer TM (2017) Steering Soil Microbiomes to Suppress Aboveground Insect Pests. *Trends in Plant Science* 22:770–778. <https://doi.org/10.1016/j.tplants.2017.07.002>
- Pineda A, Kaplan I, Hannula SE, et al (2020) Conditioning the soil microbiome through plant–soil feedbacks suppresses an aboveground insect pest. *New Phytologist* 226:595–608. <https://doi.org/10.1111/nph.16385>
- Puga-Freitas R, Blouin M (2015) A review of the effects of soil organisms on plant hormone signalling pathways. *Environmental and Experimental Botany* 114:. <https://doi.org/10.1016/j.envexpbot.2014.07.006>
- Qi G, Chen J, Chang M, et al (2018) Pandemonium Breaks Out: Disruption of Salicylic Acid-Mediated Defense by Plant Pathogens. *Molecular Plant* 11:1427–1439. <https://doi.org/10.1016/j.molp.2018.10.002>
- R Core Team (2020) R: A Language and Environment for Statistical Computing. <https://www.r-project.org/>, Vienna, Austria

- Raaijmakers J, Paulitz T, Steinberg C, et al (2009) The rhizosphere: a playground and battlefield for soilborne pathogens and beneficial microorganisms. *Plant and Soil* 321:341–361. <https://doi.org/10.1007/s11104-008-9568-6>
- Raaijmakers JM, Mazzola M (2016) Soil immune responses. *Science* 352:1392 LP – 1393. <https://doi.org/10.1126/science.aaf3252>
- Robert-Seilaniantz A, Grant M, Jones JDG (2011) Hormone crosstalk in plant disease and defense: more than just JASMONATE-SALICYLATE antagonism. *Annual Review of Phytopathology* 49:317–343. <https://doi.org/10.1146/annurev-phyto-073009-114447>
- Rolfe SA, Griffiths J, Ton J (2019) Crying out for help with root exudates: adaptive mechanisms by which stressed plants assemble health-promoting soil microbiomes. *Current Opinion in Microbiology* 49:73–82. <https://doi.org/10.1016/j.mib.2019.10.003>
- Rudrappa T, Czymmek KJ, Paré PW, Bais HP (2008) Root-Secreted Malic Acid Recruits Beneficial Soil Bacteria. *Plant Physiology* 148:1547 LP – 1556. <https://doi.org/10.1104/pp.108.127613>
- Rymaszewski W, Dauzat M, Bédiée A, et al (2018) Measurement of *Arabidopsis thaliana* Plant Traits Using the PHENOPSIS Phenotyping Platform. *Bio-protocol* 8:e2739. <https://doi.org/10.21769/BioProtoc.2739>
- Sanguin H, Sarniguet A, Gazengel K, et al (2009) Rhizosphere bacterial communities associated with disease suppressiveness stages of take-all decline in wheat monoculture. *New Phytologist* 184:694–707. <https://doi.org/10.1111/j.1469-8137.2009.03010.x>
- Schlatter D, Kinkel L, Thomashow L, et al (2017) Disease Suppressive Soils: New Insights from the Soil Microbiome. *Phytopathology*® 107:1284–1297. <https://doi.org/10.1094/PHYTO-03-17-0111-RVW>
- Steiner AA (1961) A universal method for preparing nutrient solutions of a certain desired composition. *Plant and Soil* 15:134–154. <https://doi.org/10.1007/BF01347224>
- Su F, Villaume S, Rabenoelina F, et al (2017) Different *Arabidopsis thaliana* photosynthetic and defense responses to hemibiotrophic pathogen induced by local or distal inoculation of *Burkholderia phytofirmans*. *Photosynthesis Research* 134:201–214. <https://doi.org/10.1007/s11120-017-0435-2>
- Thioulouse J, Dufour AB, Jombart T, et al (2018) Multivariate analysis of ecological data with ade4
- Trivedi P, Mattupalli C, Eversole K, Leach JE (2021) Enabling sustainable agriculture through understanding and enhancement of microbiomes. *New Phytologist* n/a: <https://doi.org/10.1111/nph.17319>
- Wang KL-C, Li H, Ecker JR (2002) Ethylene Biosynthesis and Signaling Networks . *The Plant Cell* 14:S131–S151. <https://doi.org/10.1105/tpc.001768>

Weller DM, Raaijmakers JM, Gardener BBM, Thomashow LS (2002) Microbial populations responsible for specific soil suppressiveness to plant pathogens. *Annual review of phytopathology* 40:309–48.

<https://doi.org/10.1146/annurev.phyto.40.030402.110010>

White TJ, Bruns T, Lee S, Taylor J (1990) Amplification and direct sequencing of fungal ribosomal RNA Genes for phylogenetics. In: Innis MA, Gelfand DH, Sninsky JJ, White TJB (eds) *PCR Protocols: a guide to methods and applications*. Academic Press, San Diego, pp 315–322

Yang L, Li B, Zheng X, et al (2015) Salicylic acid biosynthesis is enhanced and contributes to increased biotrophic pathogen resistance in *Arabidopsis* hybrids. *Nature Communications* 6:7309.

<https://doi.org/10.1038/ncomms8309>

Yuan J, Zhao J, Wen T, et al (2018) Root exudates drive the soil-borne legacy of aboveground pathogen infection. *Microbiome* 6:156. <https://doi.org/10.1186/s40168-018-0537-x>

#### 401 **Statements & Declarations**

#### 402 **Funding**

403 ER and RPF benefitted from an EC2CO initiative funding from CNRS. This work was also supported by the  
404 European Regional Development Fund, Project “Centre for Experimental Plant Biology” [grant no.  
405 CZ.02.1.01/0.0/0.0/16\_019/0000738] and grant from the Contact Mobility - BARRANDE Program (PHC action)  
406 awarded to LB and RPF.

407

#### 408 **Competing Interests**

409 The authors have no relevant financial or non-financial interests to disclose.

410

#### 411 **Author Contributions**

412 TK, LB, ER and RPF conceived and designed the study. TK and BJ performed the experiment. CM performed  
413 the soil DNA extraction and sequencing. RPF analysed the data. TK, MB, SJ, ER and RPF interpreted the data.  
414 TK, ER and RPF wrote the first manuscript and all authors contributed to the revision of the manuscript.

415

#### 416 **Data Availability**

417 The data that support the findings of this study are available from the corresponding author upon reasonable  
418 request.

419

## 420 **Figure legends**

421 **Fig. 1** Experimental set-up for the iterative exposure of soil microbiome to *A. thaliana* inoculated with the foliar  
422 pathogen *Pst*. Before starting the iterative process (iteration 0), plants were sown and grown for four weeks on  
423 pasteurized substrate mixed with vermicompost (providing the initial microbial inoculant). The iterative process  
424 was started (i1) by dividing the first batch of plants (i0) in two lines : i/ *pst*-line, infiltrated with a *Pst* strain, and  
425 ii/ mock-line, infiltrated with saline buffer (plain and empty red arrows respectively). This will allow to assess if  
426 the plant could recruit different microbial communities when exposed or not to a pathogen. Seven days after  
427 inoculation, disease susceptibility was assessed on the *Pst*-inoculated line. Then, for each pot of both lines, a small  
428 fraction of soil was collected and pooled with samples from the same line; an aliquot fraction of pooled soil was  
429 kept for further amplicon-based metagenomic analysis. Thus, pooled soil sample from the parental generation was  
430 used to inoculate a soil microbial community within the pasteurized substratum of the offspring one at a 1:9 (v:v)  
431 ratio to mimic the dynamics of a soil microbial community exposed to successive monocultures. *A. thaliana* seeds  
432 were sown on this inseminated soil to pursue the iterative process for eleven iterations. Each iteration is denoted  
433  $i_n$ , with n, the iteration number ranging from 1 to 11 and consisting in the three following steps: i/ sowing of  
434 *A.thaliana* on soil inoculated with the microbial community of the previous iteration. After four weeks, ii/ leaves  
435 infiltration with *Pst* strain or a saline buffer (for *pst*- and mock-line respectively). Finally, iii/ soil collection,  
436 respective to its line, to prepare a new batch of soil and pursue the iterative process. For the tenth and eleventh  
437 iteration, five additional experimental set-ups were prepared for mock lines to assess disease susceptibility while  
438 continuing the iteration process. Green and blue colours are associated with *pst*- and mock-line respectively. Red  
439 colour is associated with the pathogen *Pst* and grey colour with initial soil before starting the iterative process.  
440 Soil microbial composition has been characterized for samples indicated with asterix

441

442 **Fig. 2** Leaf traits of *Arabidopsis thaliana* along the iterative process. (a) Representative images of plants from the  
443 tenth iteration, 7 days post inoculation (d.p.i.): mock ( $MgCl_2$ ) treated (left panel) and *Pst* inoculated (right panel).  
444 Red triangles point out mock or *Pst* infiltrated leaves (empty or plain triangle respectively). White scale bar  
445 represents 10 mm. (b) Evolution of rosette area. Boxplots show the total projected leaf area at 7 d.p.i for mock  
446 (blue) or *pst* (green) lines from iteration 4 to 11 (points indicates values for biological replicates, n=8). (c) Boxplot  
447 comparing pathogen resistance of plants from mock- (n=5) or *pst*-line (n=8) at the tenth iteration (i10; points  
448 indicates values for biological replicates, see also i11 in Supplementary Fig. S1). For each plant, three leaves were

449 infiltrated with *Pst* before CFU quantification at 7 d.p.i. Asterix indicates significant differences and “ns” indicates  
450 non-significant differences (\*\*p-value < 0.01, \*p-value < 0.05, ns p-value > 0.05, Wilcoxon test)

451

452 **Fig. 3** Impact of the soil microbiome on hormone related gene expression of *Arabidopsis thaliana* from mock- or  
453 pst-line upon *Pst* infection. (a-e) SA-related, (f-h) JA-related, (i-j) ABA related and (k-l) ET related gene  
454 expression at 7 d.p.i. Data are those from iteration 10. Boxplots show Log2 transformed differential expression  
455 levels ( $\Delta\Delta Ct$ ) of the genes of interest normalized to the housekeeping gene *AtTIP41* and relative to infected plants  
456 from the mock line (points indicates values for biological replicates, n=5 and n=8 for mock-line and pst-line  
457 respectively) at the tenth iteration. Symbols indicates significant differences (\*p-value < 0.05, (.) p-value < 0.1),  
458 and “ns” indicates non-significant (p-value > 0.1) differences (Wilcoxon test)

459

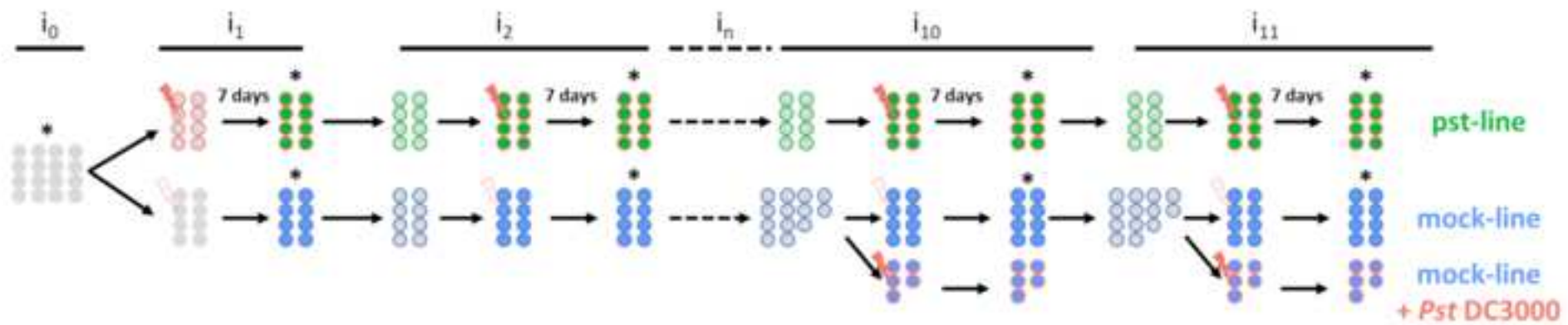
460 **Fig. 4** Legacy and *Pst* effect on bacterial and fungal community structure along the iterative process. Bray-Curtis  
461 dissimilarity (Beta-diversity) between successive iterations ( $i^{th}$  and  $(i+1)^{th}$ ) in pst- and mock-lines for bacterial (a)  
462 and fungal (b) community. Intra and inter group Bray-Curtis dissimilarity (Beta-diversity) for bacterial (c) and  
463 fungal (d) community. Green and blue solid lines represent the median (n=3) and intervals represent the minimum  
464 and maximum values for pst and mock treatment, respectively. Grey solid line represents the median (n=3) and  
465 intervals represent the minimum and maximum value of beta-diversity between pst and mock treatment

466

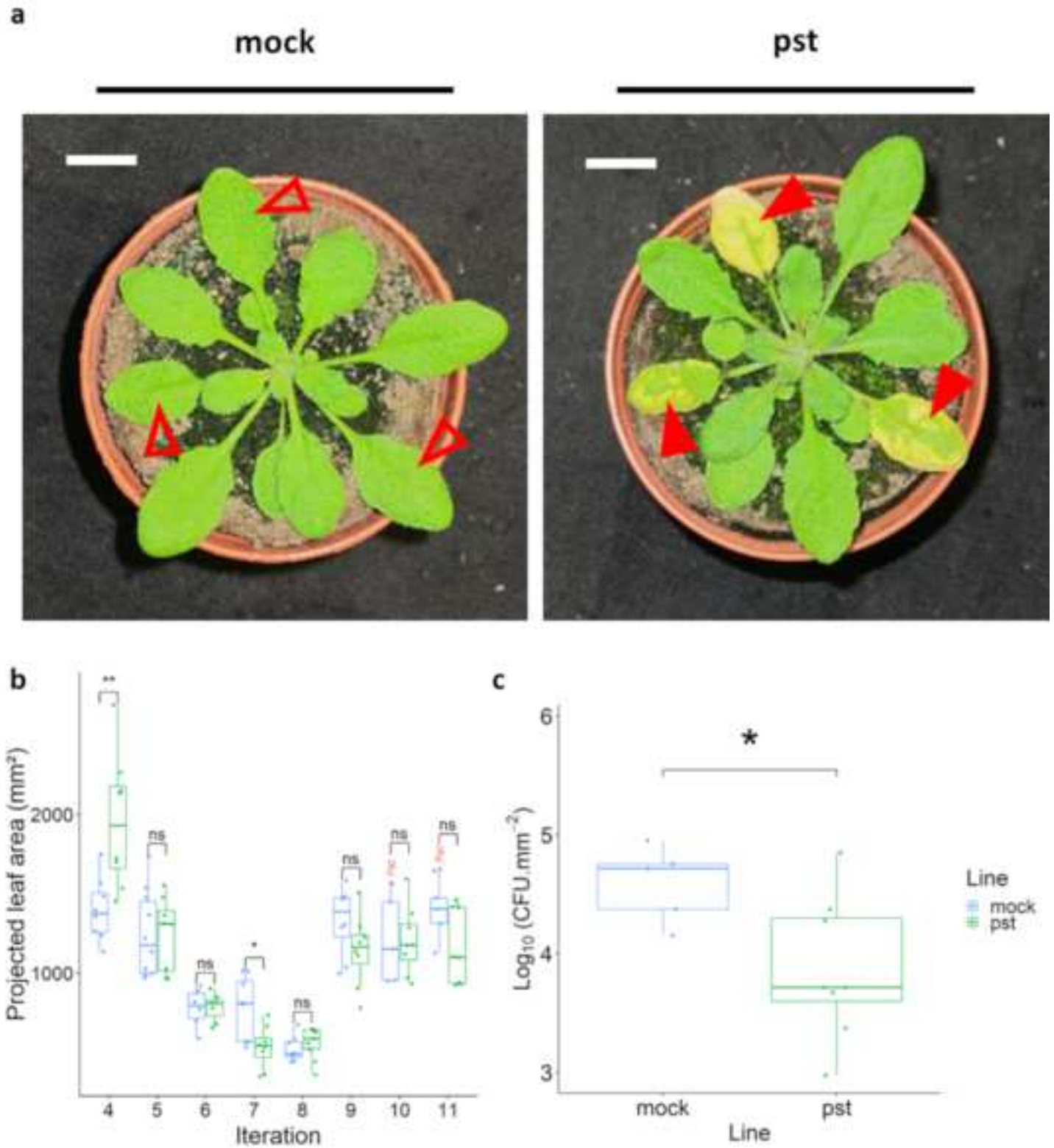
467 **Fig. 5** Community structure for bacteria along the experiment. (a) Correspondence analysis on bacterial diversity  
468 of i0 to i11. First and second axis account for 25 and 13 % of total variance respectively. (b) Correspondence  
469 analysis on bacterial diversity of iterations i8 to i11. First and second axis account for 21 and 16 % of total variance  
470 respectively. OTUs with the highest absolute contribution to the first axis are highlighted in blue and green,  
471 defining the soil bacterial sub-community of mock- and pst-lines respectively. Other OTU are shown in light grey.  
472 Symbols indicates the iteration: triangle for i8, inverted triangles for i9, squares for i10 and diamonds for i11.  
473 Mock- and pst-line barycenters are in blue and green respectively.

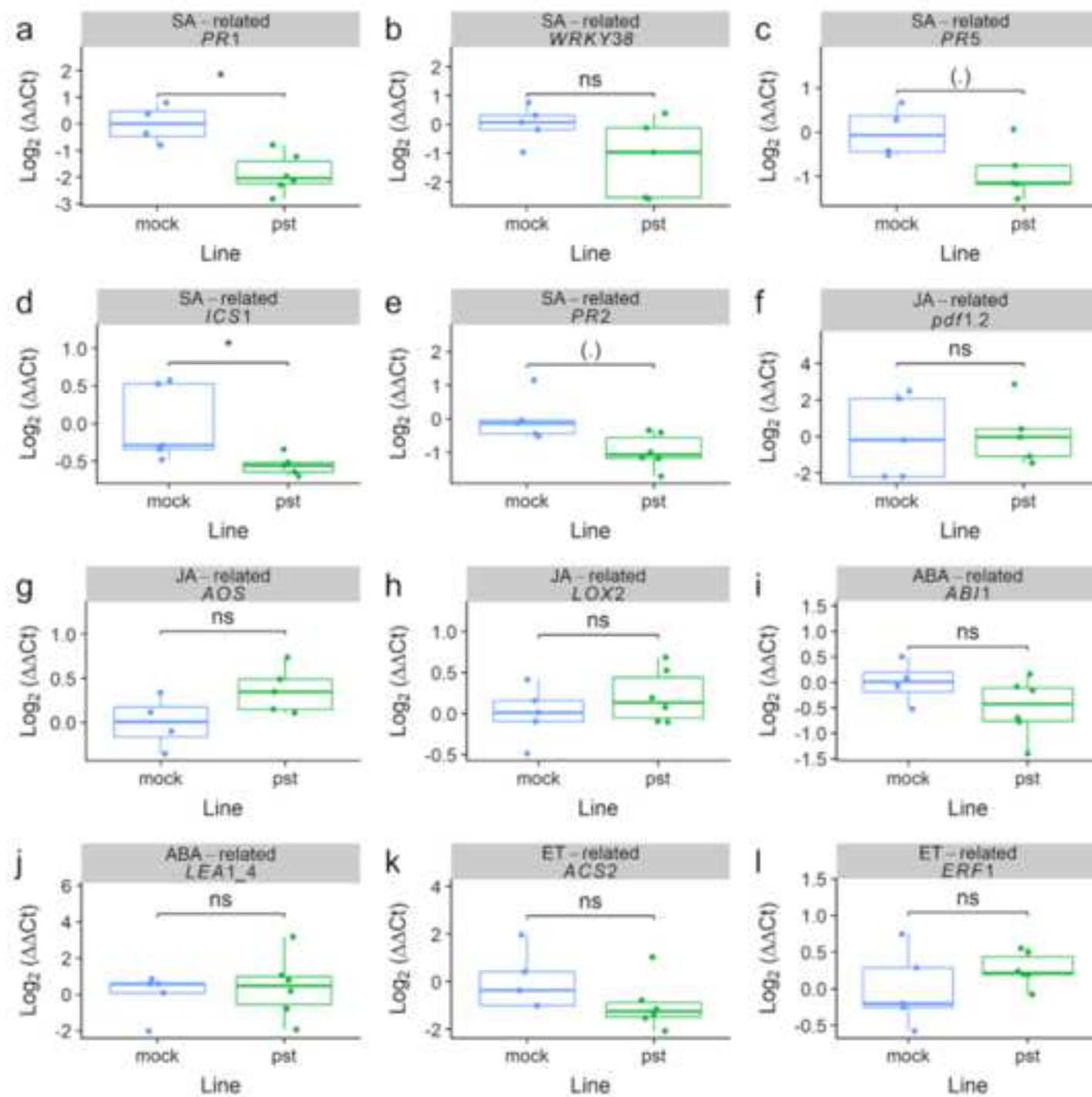
474

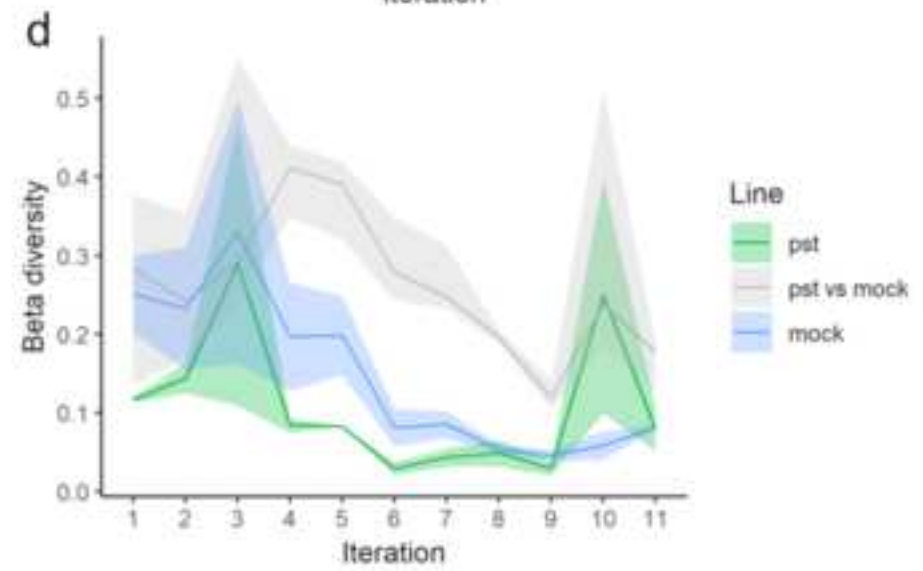
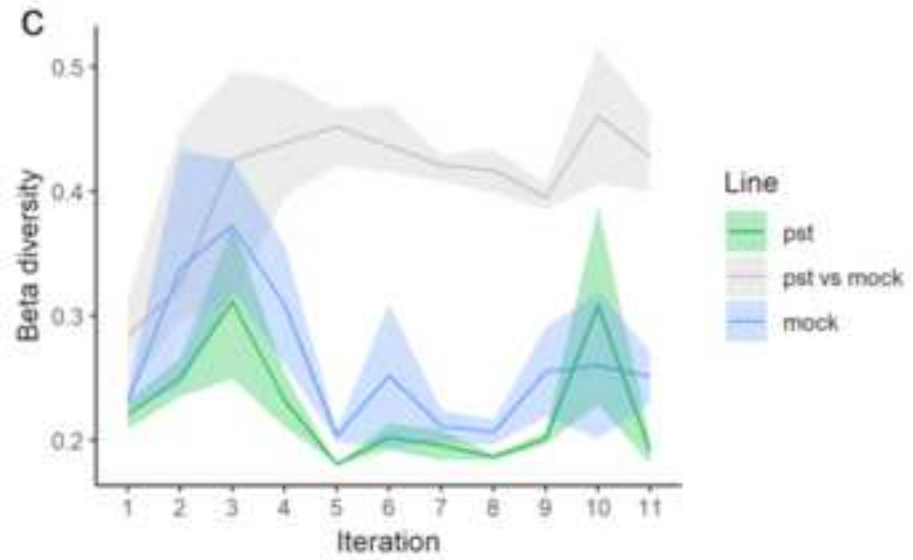
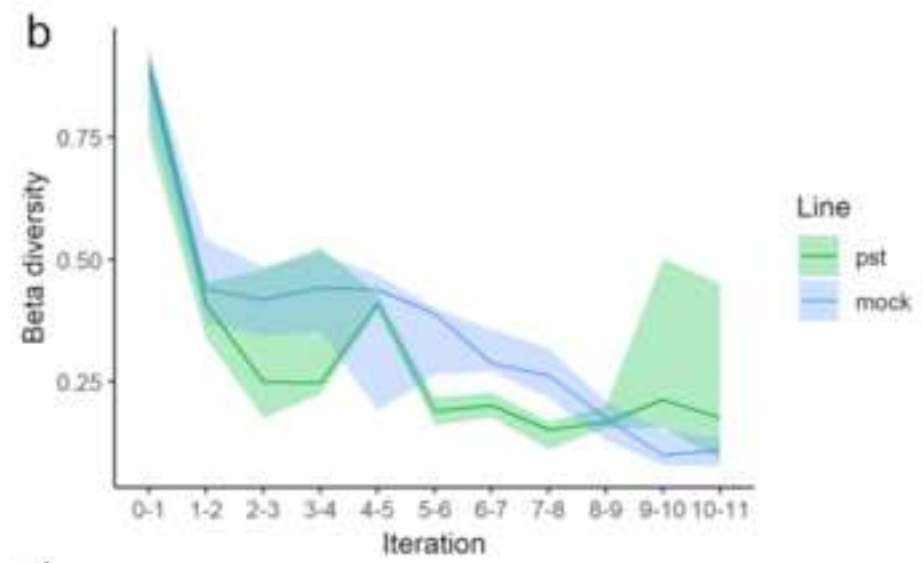
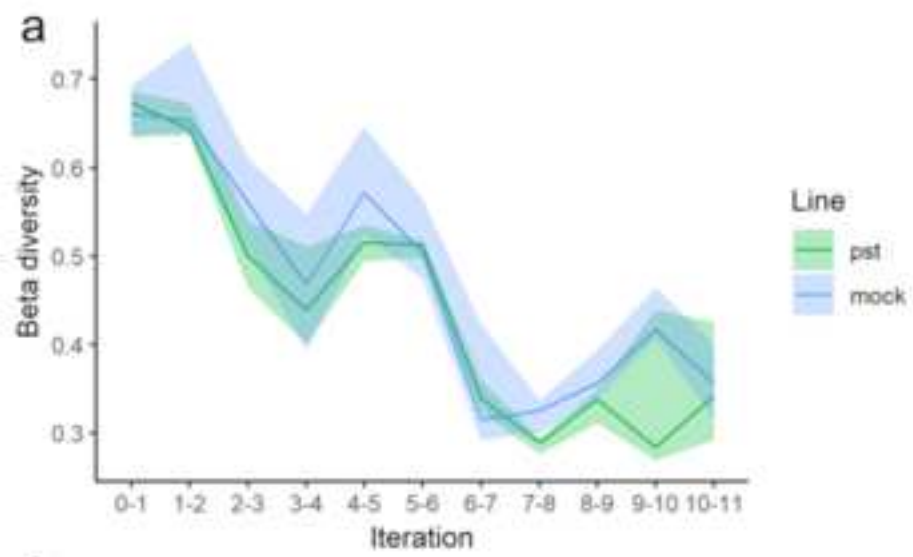
475 **Fig. 6** Main changes in the bacterial community in response to *Pst* inoculation. Relative abundance and phylum  
476 associated with (a) *Pst* treatment (78 OTUs) and (b) mock treatment (34 OTUs). Bar height represents the relative  
477 abundance (% of total abundance) of each OTU. Colour indicates taxonomic classification of OTUs at the phylum  
478 level

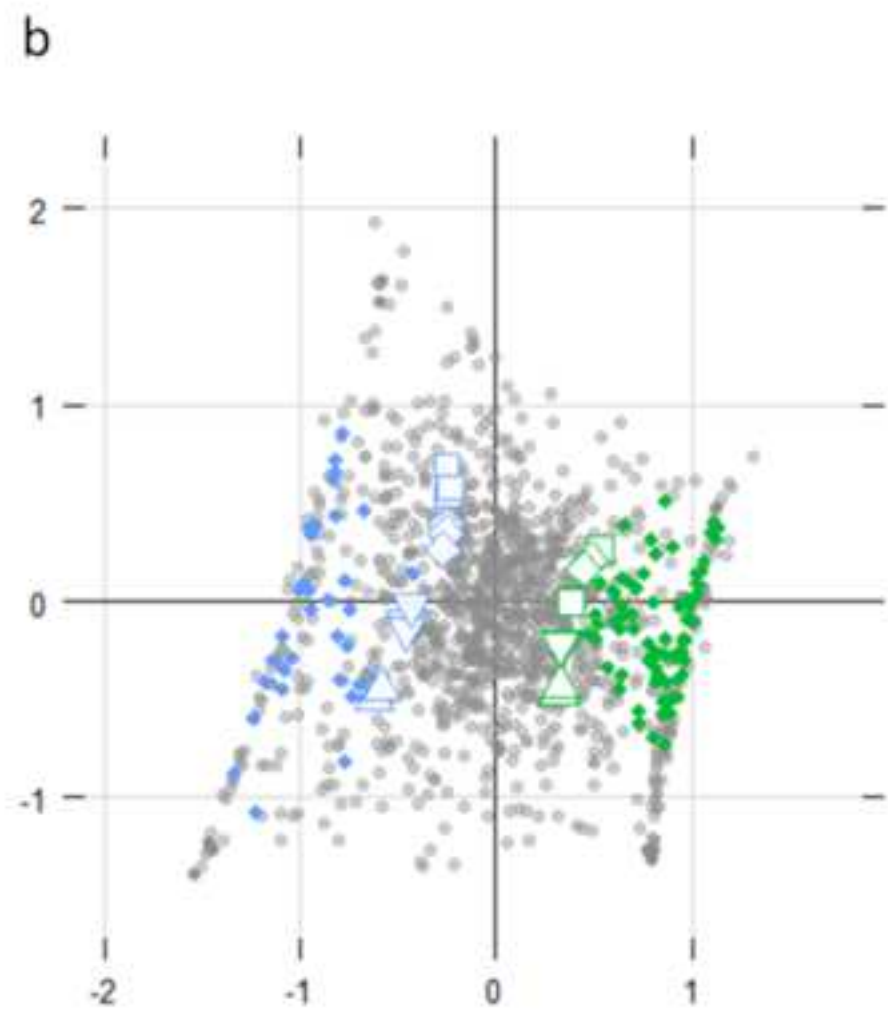
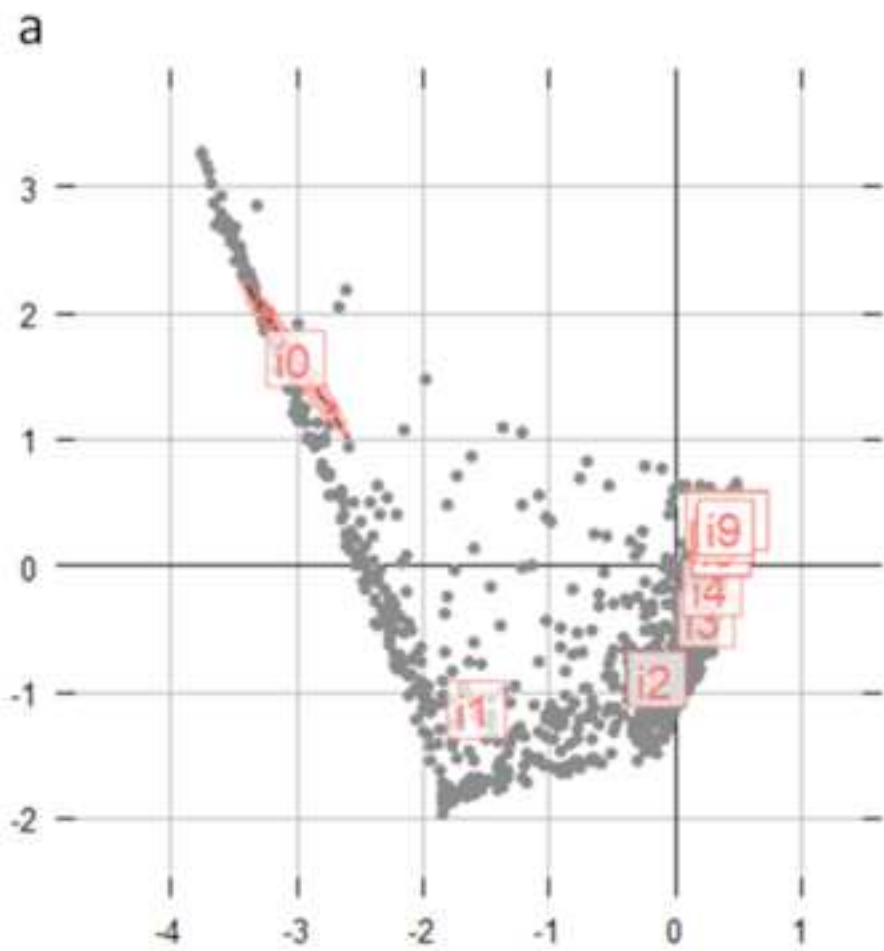


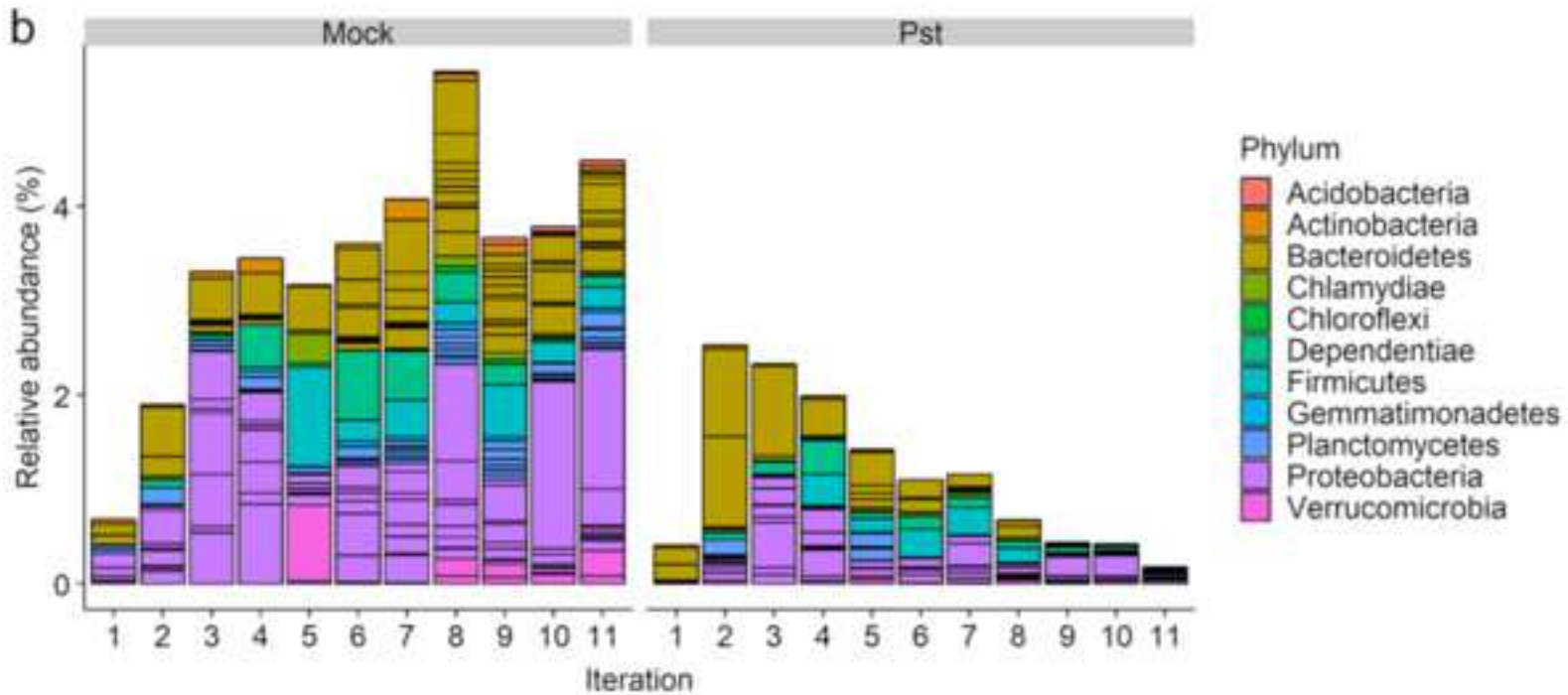
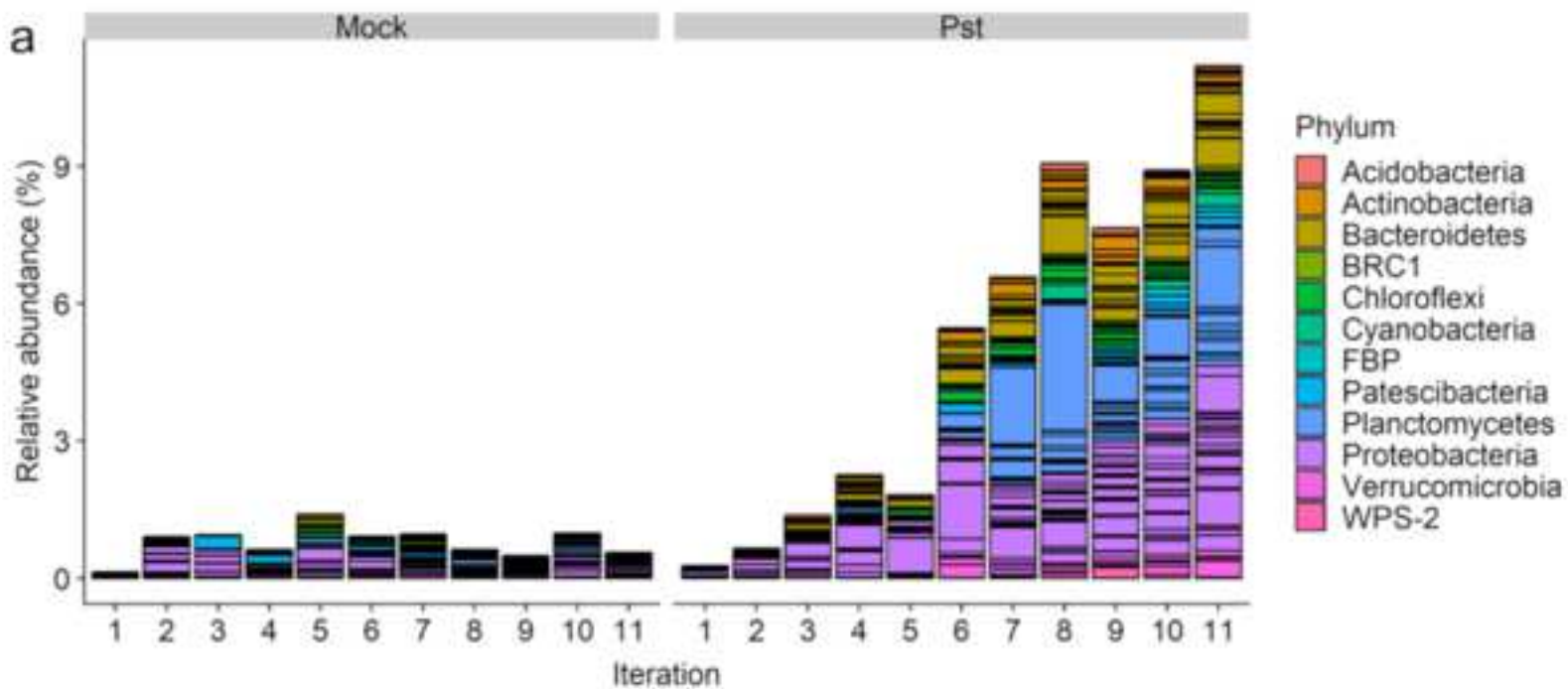


Calque copi<sup>1</sup>











Click here to access/download  
**Supplementary Material**  
ESM-1.pdf

